Robustness of the periodic and chaotic orientational behavior of tumbling nematic liquid crystals

Sebastian Heidenreich,[1,*] Patrick Ilg,[1,2] and Siegfried Hess[1]
[1]*Institute for Theoretical Physics, Technical University Berlin, Hardenbergstrasse 36, D-10623, Germany*
[2]*Université Lyon1, Laboratoire de Physique de la Matière Condensée et Nanostructures, CNRS, UMR5586, F-69622 Villeurbanne Cedex, France*
(Received 25 January 2006; published 22 June 2006)

The dynamical behavior of molecular alignment strongly affects physical properties of nematic liquid crystals. A theoretical description can be made by a nonlinear relaxation equation of the order parameter and leads to the prediction that rather complex even chaotic orientational behavior occur. Here the influence of fluctuating shear rates on the orientational dynamics especially on chaotic solutions is discussed. With the help of phase portraits and time evolution diagrams, we investigated the influence of different fluctuation strengths on the flow aligned, isotropic, and periodic solutions. To explore the effect of fluctuations on the chaotic behavior, we calculated the largest Lyapunov exponent for different fluctuation strengths. We found in all cases that small fluctuations of the shear rate do not affect the basic features of the dynamics of tumbling nematics. Furthermore, we present an amended potential modeling the isotropic to nematic transition and discuss the equivalence and difference to the commonly used Landau–de Gennes potential. In contrast to the Landau–de Gennes potential, our potential has the advantage to restrict the order parameter to physically admissible values. In the case of extensional flow, we show that the amended potential leads for increasing extensional rate to a better agreement with experimental results.

DOI: 10.1103/PhysRevE.73.061710 PACS number(s): 61.30.Cz, 61.30.Gd, 52.25.Gj

I. INTRODUCTION

Nematic liquid crystals that respond with a time-dependent orientational behavior to an applied steady shear flow rather than a stationary flow alignment are called "tumbling nematics." The time-dependent phenomena can be rather complex. Different types of periodic behavior referred to as (ordinary) tumbling, wagging, kayaking tumbling, and kayaking wagging have been identified in experiments and in theoretical descriptions [1]. A relatively simple model based on a nonlinear equation for the second rank alignment tensor [2–5] revealed a more complex and even chaotic behavior for certain model parameters and specific values of the applied shear rate [6,7]. Chaotic behavior was also found from a solution of a Fokker-Planck equation for the orientational distribution function involving 65 components rather than the five independent components of the second rank alignment tensor [8]. Further theoretical studies on the periodic and chaotic orientational and rheological behavior are presented in [9,10]. One may wonder how sensitive the solutions of the model equation are against time-dependent distortions of the applied shear rate since fluctuating contributions to the shear rate do occur in experiments. In this paper, it is demonstrated that periodic and chaotic solutions can be surprisingly robust against such distortions. At the same time we amend the previous theory based on a Landau–de Gennes free energy, which includes terms up to fourth order in the alignment tensor and which does not impose a bound on the magnitude of the alignment tensor by a version that includes arbitrary high orders and does impose a realistic bound. This point is of importance for numerical solutions, in particular, in spatially inhomogeneous situations where runaway solutions might lead to unphysically large values of the alignment. The qualitative results for the dynamic behavior obtained previously are also rather robust against the just mentioned modifications of the model equations. Of course, there are (small) quantitative changes of the parameter ranges where the various types of the orientational behavior is found.

This paper proceeds as follows. First, the relaxation equation for the alignment tensor and the constitutive equation for the pressure tensor is introduced in Secs. II A and II B, respectively. In Sec. II C, we discuss dimensionless variables and the connection of model parameters to the Ericksen-Leslie tumbling parameter. In Sec. III, we present a mean field potential modeling isotropic-to-nematic phase transition. The potential is proposed as an educated guess in Sec. III A, such that for small values of the order parameter our potential coincide with the Landau–de Gennes potential. In Sec. III B, we give a theoretical foundation for our educated guess. In Sec. IV, a specific tensor basis is introduced and the tensorial relaxation equation for the alignment tensor **a** is recast into its component form. A review of the characteristic solutions of the orientational dynamic follows in Sec. V. The performance of the mean-field potential is illustrated for the special case of planar extensional flow in Sec. VI. Section VII deals with effects of fluctuations on the orientational dynamic. We consider fluctuations of the shear rate and investigate the influence on the characteristic solutions. For that purpose, orbits in the phase space of two alignment tensor components are plotted for different fluctuation strengths and compared to the original solutions without fluctuations. To explore the affect of fluctuations on chaotic solutions, we calculate the largest Lyapunov exponent for several strengths. Finally, some conclusions are offered in Sec. VIII.

*Corresponding author. Electronic address: sebastian@itp.physik.tu-berlin.de

II. MODEL EQUATIONS

A. Relaxation equation for the alignment tensor

The alignment of liquid crystalline polymers with a molecular axis parallel to the unit vector $\mathbf{u}$ is characterized by an orientational distribution function $f(\mathbf{u},t)$. The appropriate order parameter for a nematic is the second rank alignment tensor

$$\mathbf{a} \equiv \sqrt{\frac{15}{2}}\langle\overline{\mathbf{uu}}\rangle \equiv \int f(\mathbf{u},t)\sqrt{\frac{15}{2}}\overline{\mathbf{uu}}\mathrm{d}^2u, \tag{1}$$

which is an anisotropic second moment characterizing the distribution. The symbol $\overline{\mathbf{x}}$ indicates the symmetric traceless part of a tensor $\mathbf{x}$, i.e., with Cartesian components denoted by Greek subscripts, one has $\overline{x_{\mu\nu}}=(1/2)(x_{\mu\nu}+x_{\nu\mu})-(1/3)x_{\lambda\lambda}\delta_{\mu\nu}$. Frequently, the alignment tensor is also referred to as "$\mathbf{Q}$ tensor," and sometimes as "$\mathbf{S}$ tensor."

The symmetric traceless part $\overline{\boldsymbol{\epsilon}}$ of the dielectric tensor $\boldsymbol{\epsilon}$, which gives rise to birefringence, is proportional to the alignment tensors, viz.,

$$\overline{\boldsymbol{\epsilon}} = \varepsilon_a \mathbf{a}, \tag{2}$$

with characteristic coefficient ε_a specifying the optical anisotropy. The shear flow-induced modifications of the alignment can be detected optically [11].

For the special case of uniaxial symmetry (uniaxial phase), the alignment tensor $\mathbf{a}$ can be parametrized by a scalar order parameter a and the director $\mathbf{n}$, i.e., $\mathbf{a}=a(3/2)^{1/2}\overline{\mathbf{nn}}$, such that $a^2=\mathbf{a}:\mathbf{a}$, and $-\sqrt{5}/2\le a=(3/2)^{1/2}\mathbf{a}:\overline{\mathbf{nn}}\le\sqrt{5}$. The parameter a is therefore proportional to the Maier-Saupe order parameter $S\equiv\langle P_2(\mathbf{u}\cdot\mathbf{n})\rangle=a/\sqrt{5}$, where P_2 denotes the second Legendre polynomial. Clearly, by definition, the order parameter a is bounded, just as S.

In the original theoretical approach, a nonlinear relaxation equation for the alignment tensor $\mathbf{a}$, coupled to the velocity gradient field and an expression for the contribution to the pressure or stress tensor associated with the alignment was derived [2].

The equations involve characteristic phenomenological coefficients viz. the relaxation time coefficient $\tau_{\mathbf{a}}>0$, as well as τ_{ap}, which determine the strength of the coupling between the alignment and the pressure tensor or the velocity gradient, dimensionless coefficient (shape factor) κ, and parameters for the Landau–de Gennes potential to be discussed later. These parameters are linked with the pseudocritical temperature T^*, the nematic-isotropic transition temperature T_{K} with $T_{\mathrm{K}}>T^*$, and with the value of the alignment just below T_{K}.

The equation of change for the alignment tensor $\mathbf{a}$, in the presence of a flow field $\mathbf{v}$ reads [2,5]

$$\frac{\partial\mathbf{a}}{\partial t} - 2\overline{\boldsymbol{\Omega}\times\mathbf{a}} - 2\kappa\overline{\boldsymbol{\Gamma}\cdot\mathbf{a}} + \tau_{\mathrm{a}}^{-1}\boldsymbol{\Phi}^a(\mathbf{a}) = -\sqrt{2}\frac{\tau_{\mathrm{ap}}}{\tau_{\mathrm{a}}}\boldsymbol{\Gamma}. \tag{3}$$

The symmetric traceless tensor

$$\boldsymbol{\Phi}^a(\mathbf{a}) \equiv \frac{\partial\Phi}{\partial\mathbf{a}} \tag{4}$$

is the derivative of the potential function Φ, to be specified later, with respect to the alignment tensor.

The symbols $\boldsymbol{\Gamma}$ and $\boldsymbol{\Omega}$ denote the symmetric traceless part of the velocity gradient tensor (strain rate tensor) $\boldsymbol{\Gamma}\equiv\overline{\nabla\mathbf{v}}$, and the vorticity $\boldsymbol{\Omega}\equiv(\nabla\times\mathbf{v})/2$, respectively. In the case of a simple shear flow $\mathbf{v}=\dot{\gamma}y\mathbf{e}^x$ in the x direction, gradient in the y direction, and vorticity in the z direction, to be considered throughout the following analysis, these quantities simplify to $\boldsymbol{\Gamma}=\dot{\gamma}\overline{\mathbf{e}^x\mathbf{e}^y}$ and $\boldsymbol{\Omega}=-(1/2)\dot{\gamma}\mathbf{e}^z$. The unit vectors parallel to the coordinate axes are denoted by $\mathbf{e}^x,\mathbf{e}^y,\mathbf{e}^z$.

Equation (3) has been extended to inhomogeneous systems by changing the time derivative from a partial to a substantial one, and by adding a term $\propto\triangle\mathbf{a}$ characterizing inhomogeneous systems [12], see also [13] for related works.

In the following, we focus on the homogeneous orientational behavior governed by Eq. (3) and, for simplicity, the flow field is considered like a well-controlled external field. That means we do neither study defects or other effects of inhomogeneous spatial orientational order nor the back reaction of the orientational order on the velocity.

Very recently, the present model has been extended to the case of side chain liquid crystalline polymers by introducing a second alignment tensor for the polymeric backbone [14].

In Refs. [5,7] the symbol σ was used instead of κ. The special values 0 and ±1 for the coefficient κ in Eq. (3) correspond to corotational and codeformational time derivatives. From the solution of the generalized Fokker-Planck equation one finds, for long particles, $\kappa\approx3/7\approx0.4$.

B. Constitutive relation for the pressure tensor

The alignment is not only influenced by the flow, but the flow properties as characterized by the friction pressure tensor are affected by the alignment. The full pressure tensor $\mathbf{p}$ consists of a hydrostatic pressure p, an antisymmetric part, and the symmetric traceless part $\overline{\mathbf{p}}$ referred to as friction pressure tensor [2]. The latter splits into an "isotropic" contribution as already present in fluids composed of spherical particles or in fluids of nonspherical particles in a perfectly "isotropic state" with zero alignment, and a part explicitly depending on the alignment tensor:

$$\overline{\mathbf{p}} = -2\eta_{\mathrm{iso}}\boldsymbol{\Gamma} + \overline{\mathbf{p}_{\mathrm{al}}}, \tag{5}$$

with [5]

$$\overline{\mathbf{p}_{\mathrm{al}}} = \frac{\rho}{m}k_{\mathrm{B}}T\left(\sqrt{2}\frac{\tau_{\mathrm{ap}}}{\tau_{\mathrm{a}}}\boldsymbol{\Phi}^a - 2\kappa\overline{\mathbf{a}\cdot\boldsymbol{\Phi}^a}\right). \tag{6}$$

In equilibrium, one has $\boldsymbol{\Phi}^a(\mathbf{a}_{\mathrm{eq}})=\mathbf{0}$ and, consequently, $\overline{\mathbf{p}_{\mathrm{al}}}=0$. The occurrence of the same coupling coefficient τ_{ap} in (6) as in (3) is due to Onsager symmetry relations. For studies on the rheological properties in the isotropic and nematic phases with stationary flow alignment, following from (3) and (6), see [2,5,12,15].

C. Landau–de Gennes potential and scaled variables

In previous studies [7,10], the Landau–de Gennes potential $\Phi=\Phi(\mathbf{a})$, viz.,

$$\Phi = \left(\tfrac{1}{2}\right)A(T)\mathbf{a}:\mathbf{a} - \left(\tfrac{1}{3}\right)\sqrt{6}B(\mathbf{a}\cdot\mathbf{a}):\mathbf{a} + \left(\tfrac{1}{4}\right)C(\mathbf{a}:\mathbf{a})^2 \quad (7)$$

has been used with $A(T)=A_0(1-T^*/T)$. Here A_0, B, C [with $C<2B^2/(9A_0)$] are positive dimensionless coefficients. The characteristic temperature T^* is also a model parameter. The value of A_0 depends on the proportionality coefficient chosen between $\mathbf{a}$ and $\langle\overline{\mathbf{uu}}\rangle$. The choice made in Eq. (1) implies $A_0=1$, cf. [2]. The coefficients, on the one hand, are linked with measurable quantities and, on the other hand, can be related to molecular quantities within the framework of a mesoscopic theory [16–18].

For lyotropic liquid crystals, the concentration c of nonspherical particles in a solvent rather than the temperature determines the phase transition, i.e., in this case one has $A \propto (1-c/c^*)$, where c^* is a pseudocritical concentration [17]. In Ref. [19], similar equations have been used to study the flow alignment and rheology of semidilute polymer solutions, where c^* denotes the overlap concentration.

Equations (3) and (6) can be rewritten in terms of scaled variables [2,5,12,15], which are convenient for the theoretical and numerical analysis. At the same time, the essential parameters in the system of differential equations are identified and their physical meaning is discussed. First, the alignment tensor is expressed in units of the value of the order parameter at the isotropic-nematic phase transition,

$$a_{\mathrm{K}} = \frac{2B}{3C} \quad (8)$$

occurring at the temperature $T_{\mathrm{K}}>T^*$, when the coupling coefficient D vanishes. With the reduced temperature variable

$$\vartheta \equiv \frac{9}{2}\frac{AC}{B^2} = \frac{1-T^*/T}{1-T^*/T_{\mathrm{K}}}, \quad (9)$$

the temperature dependence of the uniaxial equilibrium alignment is $a_{\mathrm{eq}}=0$ for $\vartheta \geq 9/8$ (isotropic phase) and

$$a_{\mathrm{eq}}/a_{\mathrm{K}} = \tfrac{1}{4}(3+\sqrt{9-8\vartheta}), \quad \text{for} \quad \vartheta < 9/8 \text{ (nematic phase)}. \quad (10)$$

Note that $\vartheta=1$ corresponds to the equilibrium phase coexistence temperature, for the vanishing coupling. The values $\vartheta=9/8$ and $\vartheta=0$ are the upper and lower limits of the metastable nematic and isotropic states, respectively. The quantity $\delta_{\mathrm{K}}=1-T^*/T_{\mathrm{K}}$, which sets a scale for the relative difference of the temperature from the equilibrium phase transition is known from experiments to be of the order 0.1 to 0.001. On the other hand, it is related to the coefficients occurring in the potential function according to

$$\delta_{\mathrm{K}} = \frac{2}{9}\frac{B^2}{A_0 C} = \frac{1}{2}a_{\mathrm{K}}^2\frac{C}{A_0}. \quad (11)$$

The derivative $\mathbf{\Phi}^a$ of the potential function in (3) can be written as

$$\mathbf{\Phi}^a = \Phi_{\mathrm{ref}}\mathbf{\Phi}^{a^*}(\mathbf{a}^*), \quad (12)$$

$$\Phi_{\mathrm{ref}} = a_{\mathrm{K}}\frac{2}{9}\frac{B^2}{C} = a_{\mathrm{K}}\delta_{\mathrm{K}}A_0, \quad \mathbf{a}^* = \frac{\mathbf{a}}{a_{\mathrm{K}}}, \quad (13)$$

$\mathbf{\Phi}^{\mathbf{a}^*}(\mathbf{a}^*) = \vartheta\mathbf{a}^* - 3\sqrt{6}\,\overline{\mathbf{a}^*\cdot\mathbf{a}^*} + 2\mathbf{a}^*\mathbf{a}^*:\mathbf{a}^*$. Clearly, the variable ϑ suffices to characterize the equilibrium behavior determined by $\mathbf{\Phi}^a=\mathbf{0}$. It should be mentioned that ϑ can also be interpreted as a density or concentration variable according to $\vartheta=(1-c/c^*)/(1-c_K/c^*)$, where c stands for the concentration in lyotropic liquid crystals. For the full nonequilibrium system, times and shear rates are made dimensionless with a convenient reference time. The relaxation time of the alignment in the isotropic phase is $\tau_{\mathbf{a}}A_0^{-1}(1-T^*/T)^{-1}$ showing a pretransitional increase. This relaxation time, at the coexistence temperature T_{K}, is used as a reference time

$$\tau_{\mathrm{ref}} = \tau_{\mathbf{a}}\left(\frac{1-T^*}{T_{\mathrm{K}}}\right)^{-1}A_0^{-1} = \tau_{\mathbf{a}}\delta_{\mathrm{K}}^{-1}A_0^{-1} = \tau_{\mathbf{a}}\frac{9C}{2B2} = \tau_{\mathbf{a}}a_{\mathrm{K}}\Phi_{\mathrm{ref}}^{-1}. \quad (15)$$

The shear rates are expressed in units of τ_{ref}^{-1}. The scaled shear rate, being a product of the true shear rate and the relevant relaxation time, is also referred to as "Deborah number." Instead of the ratio $\tau_{\mathrm{ap}}/\tau_{\mathbf{a}}$, the parameter

$$\lambda_{\mathrm{K}} = -\left(\frac{2}{3}\right)\sqrt{3}\frac{\tau_{\mathrm{ap}}}{\tau_{\mathbf{a}}}a_{\mathrm{K}}^{-1} \quad (16)$$

is used. As was shown previously for nematics, [5,12,16,15], the coefficients $\tau_{\mathbf{a}}$ and τ_{ap} are proportional to the Ericksen-Leslie [20] viscosity coefficients γ_1 and γ_2, respectively. The theory applies both for the isotropic and the nematic phase. The Ericksen-Leslie theory follows from this approach when the alignment tensor $\mathbf{a}\neq 0$ is uniaxial and when the effect of the shear flow on the magnitude of the order parameter can be disregarded. Then it suffices to use a dynamic equation for the "director," which is a unit vector parallel to the principal axis of the alignment tensor associated with its largest eigenvalue. This is a good approximation deep in the nematic phase and for small shear rates. For intermediate and large shear rates and, in particular, in the vicinity of the isotropic-nematic phase transition, the tensorial description is needed. The 'tumbling coefficient' $\lambda=-\gamma_2/\gamma_1=\lambda(a_{\mathrm{eq}})$ is given by

$$\lambda_{\mathrm{eq}} = \lambda_{\mathrm{K}}\frac{a_{\mathrm{K}}}{a_{\mathrm{eq}}} + \frac{1}{3}\kappa, \quad (17)$$

where a_{eq} is recalled as the equilibrium value of the alignment in the nematic phase. Thus λ_{eq} is equal to λ_{K} at the transition temperature, corresponding to $\vartheta_{\mathrm{eff}}=1$, provided that $\kappa=0$. Note that λ_{eq}, in contradistinction to λ_{K}, is defined in the nematic phase only. In the limit of small shear rates $\dot{\gamma}$, the tumbling parameter is related to the Jeffrey tumbling period [21], see also [15]. Within the Ericksen-Leslie description, the flow alignment angle χ in the nematic phase is determined by

$$\cos(2\chi) = -\gamma_1/\gamma_2 = 1/\lambda_{\mathrm{eq}}. \quad (18)$$

A stable flow alignment, at small shear rates, exists for $|\lambda_{\mathrm{eq}}|>1$ only. For $|\lambda_{\mathrm{eq}}|<1$ tumbling and an even more complex time-dependent behavior of the orientation occur. The

quantity $|\lambda_{eq}|-1$ can change sign as function of the variable ϑ. For $|\lambda_{eq}|<1$ and in the limit of small shear rates $\dot{\gamma}$, the Jeffrey tumbling period [21] is related to the Ericksen-Leslie tumbling parameter λ_{eq} by $P_J=\frac{4\pi}{\dot{\gamma}\sqrt{1-\lambda_{eq}^2}}$, for a full rotation of the director.

In the following, λ_K and κ are considered as model parameters. The first one is essential for the coupling between the alignment and the viscous flow. The coefficients κ influence the orientational behavior quantitatively but do not seem to affect it in a qualitative way. If one wants to correlate the present theory with the flow behavior of the alignment in the isotropic phase, on the one hand, and in the nematic phase, on the other hand, for small shear rates where the magnitude of the order parameters is practically not altered, it suffices to study the case $\lambda_K\neq 0$, $\kappa=0$, in order to match an experimental value of λ by the expression (17). Mesoscopic theories [16,18,22] indicate that $\kappa\sim\lambda_K$. Thus, the case $\kappa\neq 0$, in particular $\kappa=0.4$, is also studied.

D. Scaled variables: stress tensor

The stress tensor (6) associated with the alignment is related to the relevant quantities expressed in terms of scaled variables by

$$-\overline{\mathbf{p}_{al}}=\sqrt{2}\frac{\rho}{m}k_BTa_K\Phi_{ref}\frac{\sqrt{3}}{2}\lambda_K\tilde{\mathbf{\Phi}}^a, \tag{19}$$

$$\tilde{\mathbf{\Phi}}^a=\mathbf{\Phi}^{a^*}+\frac{2\kappa}{3\lambda_K}\sqrt{6}\overline{\mathbf{a}^*\cdot\mathbf{\Phi}^{a^*}}, \tag{20}$$

where $\mathbf{a}^*=\mathbf{a}/a_K$ and $\mathbf{\Phi}^{a^*}=\mathbf{\Phi}^a/\Phi_{ref}$ in [15], [23]. The dimensionless shear stress $\mathbf{\Sigma}^{al}$ associated with the alignment is defined by

$$\mathbf{\Sigma}^{al}\equiv\frac{2}{\sqrt{3}}\lambda_K^{-1}\tilde{\mathbf{\Phi}}^a. \tag{21}$$

Then, Eq. (19) is equivalent to

$$-\overline{\mathbf{p}_{al}}=\sqrt{2}G_{al}\mathbf{\Sigma}^{al},\quad G_{al}=\frac{3}{4}\frac{\rho k_BT}{m}\lambda_K^2\delta_KA_0a_K^2, \tag{22}$$

where G_{al} is a shear modulus associated with the alignment contribution to the stress tensor, and the product $A_0a_K^2$ is essentially one parameter entering the theoretical expressions. The quantity $\eta_{ref}=G_{al}\tau_{al}$ serves as a reference value for the viscosity. With the scaling used here, the dimensionless (first) Newtonian viscosity, in the isotropic phase, is $\eta_{New}^*=1+\eta_{iso}^*$ with $\eta_{iso}^*=\eta_{iso}/\eta_{ref}$. For high shear rates, the dimensionless viscosity η^* approaches the second Newtonian viscosity η_{iso}^*. The total deviatoric (symmetric traceless) part of the stress tensor, in units of G_{al}, is denoted by σ. In terms of the quantities introduced here it is given by, cf. (5),

$$G_{al}\sigma=-\overline{\mathbf{p}}=2\eta_{iso}\mathbf{\Gamma}-\overline{\mathbf{p}_{al}}=2\eta_{iso}\mathbf{\Gamma}+\sqrt{2}G_{al}\mathbf{\Sigma}^{al}. \tag{23}$$

In the same way the relaxation equation [Eq. (3)] of the alignment tensor can be scaled as

$$\frac{\partial\mathbf{a}^*}{\partial t^*}-2\overline{\mathbf{\Omega}^*\times\mathbf{a}^*}-2\kappa\overline{\mathbf{\Gamma}^*\cdot\mathbf{a}^*}+\mathbf{\Phi}^a(\mathbf{a}^*)=\sqrt{\frac{3}{2}}\lambda_k\mathbf{\Gamma}^*. \tag{24}$$

Here, we used the dimensionless time $t^*=t\tau_{ref}^{-1}$, Γ^* and Ω^* as the symmetric traceless and antisymmetric part of the dimensionless velocity gradient $\nabla^*\mathbf{v}^*$. In the case of plane Couette flow $\nabla^*\mathbf{v}^*$ is equal to the dimensionless shear rate $\dot{\gamma}^*=\dot{\gamma}\tau_{ref}$.

In the following, we will denote quantities in reduced units by the same symbols as the original ones, unless ambiguities could arise.

III. AMENDED POTENTIAL FUNCTION

A. An educated guess

It is convenient to formulate the amended potential function in terms of the scaled variables introduced above. Furthermore, the expansion of the potential in terms of the alignment should reduce to the Landau–de Gennes expression (7) when terms of higher than fourth order are disregarded. Thus, the ansatz

$$\Phi=\left(\tfrac{1}{2}\right)\vartheta\mathbf{a}:\mathbf{a}-\sqrt{6}(\mathbf{a}\cdot\mathbf{a}):\mathbf{a}+\varphi \tag{25}$$

is made where φ should reduce to $(1/2)(\mathbf{a}:\mathbf{a})^2$ for small values of the alignment. As mentioned, it is understood that $\mathbf{a}$ and $\mathbf{\Phi}$ stand for $\mathbf{a}^*$ and $\mathbf{\Phi}^*$. A simple choice for φ, which ensures that the magnitude of the alignment does not exceed a_{max}, is

$$\varphi=-\left(\frac{1}{2}\right)a_{max}^4\ln\left(1-\frac{(\mathbf{a}:\mathbf{a})^2}{a_{max}^4}\right). \tag{26}$$

In the case of a uniaxial alignment where one has $\mathbf{a}=a(3/2)^{1/2}\overline{\mathbf{nn}}$, the potential function reduces to a function of the scalar order parameter a, viz.,

$$\Phi=\left(\frac{1}{2}\right)\vartheta a^2-a^3-\left(\frac{1}{2}\right)a_{max}^4\ln\left(1-\frac{a^4}{a_{max}^4}\right). \tag{27}$$

In the following, $a_{max}=2.5$ is chosen. This is a plausible value for thermotropic liquid crystals, where the Maier-Saupe order parameter $S=\langle P_2\rangle$ is about 0.4 at the transition temperature. Thus, the maximum value 1 for S is larger by the factor 2.5. In the Landau–de Gennes case, one has $a=a_K=1$ at the transition temperature $\vartheta=\vartheta_K=1$. For the amended potential with $a_{max}=2.5$, one has the transition at $\vartheta=\vartheta_K\approx 0.9883$ with $a_K\approx 0.9667$. Because of the small difference between these values, it is convenient to maintain the Landau–de Gennes scaling for the physical variables.

The amended potential function (27), for the uniaxial case, is compared to the Landau–de Gennes potential in Fig. 1. The difference of the amended potential to the Landau–de Gennes potential near the pseudocritical temperature $\vartheta=0$ is very small for $a\lesssim 1$, so that the same dynamical solutions at nearly the same model parameter $\dot{\gamma},\lambda_K$ for $\vartheta=0$ can be found with a slightly shifted value of the tumbling parameter value λ_K as expressed in Fig. 2.

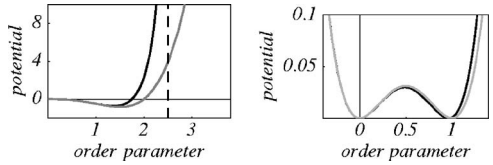

FIG. 1. The Landau–de Gennes potential (gray line) and the amended potential (dark line) as a function of the scalar order parameter a for $\vartheta=0$ (left) and $\vartheta=1$ (right).

B. Theoretical foundation

Based on Onsager's excluded volume model of hard rods, the first-order corrections to the Maier-Saupe mean field potential were calculated in [24]. Here, we show that the second- and higher-order corrections lead to a restriction of the order parameter.

The Fokker-Planck equation for the probability distribution function $f(\mathbf{u},t)$ in the presence of a flow field was given independently by Hess [16] and Doi [18], viz.,

$$\partial_t f = -\boldsymbol{\mathcal{L}}\cdot[\mathbf{u}\times(\mathbf{k}\cdot\mathbf{u}f)] + \boldsymbol{\mathcal{L}}\cdot D_r f \boldsymbol{\mathcal{L}}\left(\frac{\delta A}{\delta f(\mathbf{u})}\right). \quad (28)$$

Here, $\boldsymbol{\mathcal{L}}=\mathbf{u}\times\frac{\partial}{\partial\mathbf{u}}$ is the rotational operator, $\frac{\partial}{\partial\mathbf{u}}$ the derivative on the unit sphere, $\mathbf{k}=\nabla\mathbf{v}$ the velocity gradient, D_r the rotational diffusion constant, and $\frac{\delta A}{\delta f}$ the functional derivative of $A=A_0+A_1$, the free energy per molecule modulo k_BT. The free energy consists of the loss of entropy with molecular alignment

$$A_0 = \ln\nu - 1 + \langle\ln f(\mathbf{u})\rangle \quad (29)$$

and the Onsager free energy of steric interaction in the second virial approximation

$$A_1 = \frac{U}{2}\langle\langle\sqrt{1-(\mathbf{u}\cdot\mathbf{w})^2}\rangle\rangle, \quad (30)$$

where $U=2bL^2\nu$ is the reduced excluded volume, $2b$ and L are the diameter and the length of the rodlike molecules, and ν is the number of molecules per unit volume. Here and below, we use the following notation for averages of arbitrary functions $F(\mathbf{u})$: $\langle F(\mathbf{u})\rangle=\int F(\mathbf{u})f(\mathbf{u})d\mathbf{u}$ and $\langle\langle F(\mathbf{u},\mathbf{w})\rangle\rangle=\int\int F(\mathbf{u},\mathbf{w})f(\mathbf{u})f(\mathbf{w})d\mathbf{u}d\mathbf{w}$.

In principle, a hierarchy of moment equations can be derived from the Fokker-Planck equation (28). However, because of the nonlinearity of A_1, the time evolution equation of the alignment tensor $\mathbf{a}$ couples directly to all higher-order moments, which makes further analytical studies impractical. In [24], systematic approximations to the functional A_1 have been proposed that lead to simpler hierarchies of moment equations, which can be further analyzed. The first and second terms in the approximation $A_1\approx A_1^{(1)}+A_1^{(2)}$ are [24]

$$A_1^{(1)} = \frac{U}{2}\sqrt{1-\langle\mathbf{uu}\rangle:\langle\mathbf{uu}\rangle} \quad (31)$$

$$A_1^{(2)} = -\frac{U}{16}\langle\langle[(\mathbf{u}\cdot\mathbf{w})^2-\langle\mathbf{uu}\rangle:\langle\mathbf{uu}\rangle]^2\rangle\rangle(1-\langle\mathbf{uu}\rangle:\langle\mathbf{uu}\rangle)^{-(3/2)}. \quad (32)$$

The functional derivative of $A_1^{(1)}$ and $A_1^{(2)}$ are derived as

$$\frac{\delta}{\delta f}A_1^{(1)} = \frac{U\mathbf{uu}:\langle\mathbf{uu}\rangle}{2\sqrt{1-\langle\mathbf{uu}\rangle:\langle\mathbf{uu}\rangle}} \quad (33)$$

$$\frac{\delta}{\delta f}A_1^{(2)} = -\frac{U}{8}\frac{\mathbf{uuuu}::\langle\mathbf{uuuu}\rangle-2(\mathbf{uu}:\langle\mathbf{uu}\rangle)(\langle\mathbf{uu}\rangle:\langle\mathbf{uu}\rangle)}{(1-\langle\mathbf{uu}\rangle:\langle\mathbf{uu}\rangle)^{3/2}}. \quad (34)$$

By Prager's procedure, the relaxation of the alignment tensor $\mathbf{a}$ can be derived form Eqs. (28), (31), and (32), viz.,

$$\begin{aligned}\partial_t\mathbf{a} = {} & D_r\left(\langle\boldsymbol{\mathcal{L}}\cdot\boldsymbol{\mathcal{L}}\mathbf{t}\rangle - \frac{\mathbf{U}}{2\sqrt{\mathbf{1}-\langle\mathbf{uu}\rangle:\langle\mathbf{uu}\rangle}}\langle(\boldsymbol{\mathcal{L}}\mathbf{t})\cdot\boldsymbol{\mathcal{L}}\mathbf{uu}:\langle\mathbf{uu}\rangle\rangle\right)\\ & + D_r\frac{U}{\sqrt{(1-\langle\mathbf{uu}\rangle:\langle\mathbf{uu}\rangle)^{\mathbf{3}}}}\left(\frac{1}{4}\langle(\boldsymbol{\mathcal{L}}\mathbf{t})\cdot\boldsymbol{\mathcal{L}}\mathbf{uu}:\langle\mathbf{uu}\rangle\rangle\right)\\ & + \frac{\mathbf{1}}{\mathbf{8}}\langle(\boldsymbol{\mathcal{L}}\mathbf{t})\cdot\boldsymbol{\mathcal{L}}\mathbf{uuuu}::\langle\mathbf{uuuu}\rangle\rangle, \end{aligned} \quad (35)$$

where $\mathbf{a}=\langle\mathbf{t}\rangle$ and $\mathbf{t}=\overline{\mathbf{uu}}$. We use the decoupling approximations $\mathbf{a}:\langle\mathbf{uuuu}\rangle=\mathbf{a}:\langle\mathbf{uu}\rangle\langle\mathbf{uu}\rangle$, $\langle\mathbf{uuuu}\rangle::\langle\mathbf{uuuu}\rangle=\langle\mathbf{uu}\rangle\langle\mathbf{uu}\rangle::\langle\mathbf{uuuu}\rangle$ and consider the uniaxial case $\mathbf{a}=q\overline{\mathbf{nn}}$, where $q=\sqrt{\frac{3}{2}}a$. The relaxation equation for the scalar order parameter q is derived as

$$\partial_t q = -6D_r\frac{\partial\phi(q,U)}{\partial S},$$

$$\begin{aligned}\phi(q,U) = {} & \frac{q^2}{2} - \frac{U'}{6}\sqrt{1-q^2}\left(1-\frac{3q}{2}+2q^2\right) - \frac{U'}{4}\arcsin(q)\\ & + \frac{U'}{6} + \frac{U'}{\sqrt{(1-q^2)^3}}\left(-\frac{1}{4}q^7+\frac{1}{12}q^6-\frac{3}{16}q^5+\frac{1}{4}q^4\right.\\ & \left.+\frac{21}{16}q^3-\frac{15}{16}q^2-\frac{7}{8}q+\frac{29}{48}[1-\sqrt{(1-q^2)^3}]\right)\\ & + \frac{7}{8}\arcsin(q). \end{aligned} \quad (36)$$

The integration constant is determined by the requirement $\Phi(0)=0$. In addition to the first corrections calculated in [24], the second correction terms are singular for $q\to\pm1$. Hence, the use of approximations to Onsager's excluded volume potential leads to a restriction of the order parameter values in a natural way. This important point was missed in the original presentation and subsequent studies, where the Onsager potential was replaced by the Maier-Saupe potential. It is interesting to note, that taking into account higher-order corrections does not change the singularity since these terms produce higher-order derivatives of $\sqrt{1-\mathbf{u}\cdot\mathbf{w}}$. Note also that, although the use of different decoupling schemes lead to different forms of the potential (36), the singularity for $q\to\pm1$ remains unchanged. The order parameter q is related to the Maier-Saupe order parameter by $q=\sqrt{\frac{15}{2}}S$. The

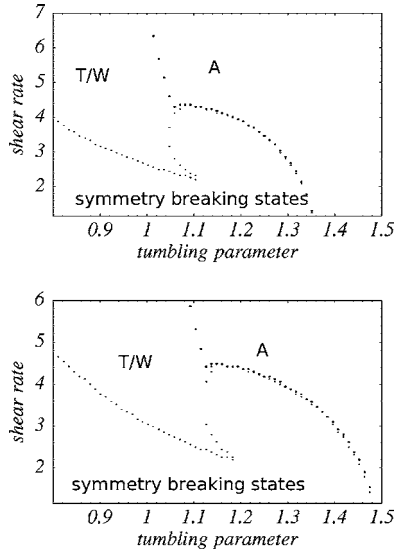

FIG. 2. The rheological phase plot is shown for flow alignment (A), in-plane (T/W), and out-plane regimes (symmetry breaking states). In the upper panel, the amended potential and in the lower panel the Landau–de Gennes potential was used. The reduced temperature is $\vartheta=0$ and the parameter $\kappa=0$.

full tensorial form of (36) is difficult to receive, and hence, we use for further analyses the simple potential (25) with $a_{\max}=2.5$.

IV. BASIS TENSORS AND COMPONENT NOTATION

The symmetric traceless alignment tensor has five independent components. It can be expressed in a standard [25] orthonormalized tensor basis as follows:

$$\mathbf{a}=\sum_{k=0}^{4} a_k\mathbf{T}^k, \quad \mathbf{T}^0\equiv\sqrt{3/2}\,\overline{\mathbf{e}^z\mathbf{e}^z}, \quad \mathbf{T}^1\equiv\sqrt{1/2}(\mathbf{e}^x\mathbf{e}^x-\mathbf{e}^y\mathbf{e}^y),$$

$$\mathbf{T}^2\equiv\sqrt{2}\,\overline{\mathbf{e}^x\mathbf{e}^y}, \quad \mathbf{T}^3\equiv\sqrt{2}\,\overline{\mathbf{e}^x\mathbf{e}^z}, \quad \mathbf{T}^4\equiv\sqrt{2}\,\overline{\mathbf{e}^y\mathbf{e}^z}, \quad (37)$$

where $\mathbf{T}^i$ with $i=0,\ldots,4$ are the basis tensors by which $\mathbf{a}$ is uniquely expressed. The orthogonality relation and the expression for the coefficients a_k are given by $\mathbf{T}^i:\mathbf{T}^k=\delta_{ik}$ and $a_i=\mathbf{a}:\mathbf{T}^i$.

Using these basis tensors, one obtains from Eq. (24) a system of ordinary differential equations

$$\dot{a}_0=-\Phi_0^a-\tfrac{1}{3}\sqrt{3}\kappa\dot{\gamma}a_2, \quad \dot{a}_1=-\Phi_1^a+\dot{\gamma}a_2,$$

$$\dot{a}_2=-\Phi_2^a-\dot{\gamma}a_1+\tfrac{\sqrt{3}}{2}\lambda_{\mathrm{K}}\dot{\gamma}-\tfrac{1}{3}\sqrt{3}\kappa\dot{\gamma}a_0,$$

$$\dot{a}_3=-\Phi_3^a+\tfrac{1}{2}\dot{\gamma}(\kappa+1)a_4, \quad \dot{a}_4=-\Phi_4^a+\tfrac{1}{2}\dot{\gamma}(\kappa-1)a_3, \quad (38)$$

where $\Phi_i^a\equiv\mathbf{\Phi}^a:\mathbf{T}^i$ is given by

$$\Phi_0^a=(\vartheta-3a_0+2a^2\psi)a_0+3(a_1^2+a_2^2)-\tfrac{3}{2}(a_3^2+a_4^2),$$

$$\Phi_1^a=(\vartheta+6a_0+2a^2\psi)a_1-\tfrac{3}{2}\sqrt{3}(a_3^2-a_4^2),$$

$$\Phi_2^a=(\vartheta+6a_0+2a^2\psi)a_2-3\sqrt{3}a_3a_4,$$

$$\Phi_3^a=(\vartheta-3a_0+2a^2\psi)a_3-3\sqrt{3}(a_1a_3+a_2a_4),$$

$$\Phi_4^a=(\vartheta-3a_0+2a^2\psi)a_4-3\sqrt{3}(a_2a_3-a_1a_4). \quad (39)$$

The notation $a^2\equiv a_0^2+a_1^2+a_2^2+a_3^2+a_4^2$ is used. The quantity ψ is equal to 1 for the Landau–de Gennes potential and

$$\psi=\left(1-\frac{(a^2)^2}{a_{\max}^4}\right)^{-1} \quad (40)$$

for the amended potential function (25) used here. The parameters $\vartheta,\lambda_{\mathrm{K}},\kappa$ were introduced in Sec. II.

The corresponding expansion with respect to the basis tensors and the component notation can be used for the other second rank irreducible tensors. From Eqs. (21) and (19), one deduces expressions for the (dimensionless) shear stress σ_{xy}, and the normal stress differences $N_1=\sigma_{xx}-\sigma_{yy}$ and $N_2=\sigma_{yy}-\sigma_{zz}$ in terms of the dimensionless tensor components $\Sigma_i\equiv\mathbf{\Sigma}^{\mathrm{al}}:\mathbf{T}^i$. These relations are

$$\sigma_{xy}=\eta_{\mathrm{iso}}\dot{\gamma}+\Sigma_2, \quad N_1=2\Sigma_1, \quad N_2=-\sqrt{3}\Sigma_0-\Sigma_1, \quad (41)$$

with

$$\Sigma_2=\frac{2}{\sqrt{3}\lambda_{\mathrm{K}}}\left[\Phi_2^a-\tilde{\kappa}\left(a_2\Phi_0^a+a_0\Phi_2^a-\frac{\sqrt{3}}{2}(a_4\Phi_3^a+a_3\Phi_4^a)\right)\right],$$

$$\Sigma_1=\frac{2}{\sqrt{3}\lambda_{\mathrm{K}}}\left[\Phi_1^a-\tilde{\kappa}\left(a_1\Phi_0^a+a_0\Phi_1^a-\frac{\sqrt{3}}{2}(a_3\Phi_3^a-a_4\Phi_4^a)\right)\right],$$

$$\Sigma_0=\frac{2}{\sqrt{3}\lambda_{\mathrm{K}}}\left[\Phi_0^a-\tilde{\kappa}\left(a_0\Phi_0^a-a_1\Phi_1^a-a_2\Phi_2^a+\frac{1}{2}(a_3\Phi_3^a+a_4\Phi_4^a)\right)\right], \quad (42)$$

and $\tilde{\kappa}=2\kappa/(3\lambda_{\mathrm{K}})$.

V. REVIEW OF CHARACTERISTIC SOLUTIONS FOR ORIENTATIONAL DYNAMICS

Depending on the relevant model parameters $\dot{\gamma},\lambda_{\mathrm{K}},\kappa,\vartheta$, the solutions of the dynamic equations (38) with (39) for the alignment tensor components either approach a steady state or are time dependent when a stationary shear rate is imposed. Furthermore, solutions that, for long times, maintain the symmetry of the plane Couette-type velocity gradient and where the tensor components a_3 and a_4 vanish have to be distinguished from symmetry-breaking solutions where these components are nonzero. The latter ones are also referred to as "out-of-plane" solutions, in contradistinction to the "in-plane" states where the "main" director, i.e., the axis associated with the largest eigenvalue of the alignment tensor, is in the flow plane determined by the direction of the flow and its gradient. The following types of orbits have been found [7].

(i) Symmetry-adapted states with $a_3=a_4=0$, which comprise *aligning* (A), stationary in-plane flow alignment with

$a_0<0$; *tumbling* (T), in-plane tumbling of the alignment tensor (i.e., the main director is in the flow plane and rotates about the vorticity axis); *wagging* (W), in-plane wagging or librational motion of the main director about the flow direction; and *log-rolling*, stationary alignment with $a_1=a_2=0$ and $a_0>0$. This out-of-plane solution is instable, in most cases.

(ii) Symmetry-breaking states with $a_3\neq 0$, $a_4\neq 0$, more specifically: *stationary symmetry-breaking states*, which occur in pairs of a_3, a_4 and $-a_3$, $-a_4$; *kayaking tumbling* (KT), the projection of the main director onto the flow plane describes a tumbling motion; *kayaking wagging* (KW), a periodic orbit where the projection of the main director onto the flow plane describes a wagging motion; and *complex* (C), complicated motion of the alignment tensor. This includes periodic orbits composed of sequences of KT and KW motion with multiple periodicity as well as aperiodic, erratic orbits. The largest Lyapunov exponent for the latter orbits is positive, i.e., these orbits are *chaotic*.

For a given choice of parameters, in general, only a subset of these solutions are found by increasing the shear rate $\dot{\gamma}$. The type of orientational behavior strongly affects the rheological behavior of the fluid. In the following, results for the orientational behavior are presented as functions of the shear rate and of the strength of its fluctuating part for a few selected values for the temperature and for the other model parameters λ_K and κ.

VI. EXTENSIONAL FLOW

As discussed earlier, terms of higher than fourth order are disregarded in the Landau–de Gennes potential even though these terms are important in order to restrict the range of values of the order parameter. For extensional flows, in particular, this fact becomes significant. Maffettone *et al.* [26] analyzed the extensional flow of a two-dimensional nematic polymer. From the numerical solution $f(\mathbf{u})$ of the corresponding Fokker-Planck equation, these authors calculated the value of the order parameter as a function of the extension rate. Within this approach, the values of the order parameter are calculated from $f(\mathbf{u})$ via Eq. (1) and naturally obey the physical bounds.

The momentum equation for the alignment tensor including the Landau–de Gennes potential, however, does not restrict the values of the orientational order parameter for extensional flows. Here we show that the dynamical equation with the amended potential proposed in Sec. III A restricts the order parameter in a satisfying form.

For planar extensional flows in the x direction and an extensional rate $\dot{\epsilon}$, the strain tensor can be written as $\mathbf{\Gamma}=\mathrm{diag}(\dot{\epsilon},-\dot{\epsilon},0)$, and therefore, the dynamics of the alignment tensor components in the tensor basis (37) are given by

$$\dot{a}_0=-\Phi_0^a-\tfrac{2}{\sqrt{3}}\kappa\dot{\epsilon}a_1 \tag{43}$$

$$\dot{a}_1=-\Phi_1^a+\sqrt{3}\lambda_K\dot{\epsilon}-\tfrac{2}{\sqrt{3}}\kappa\dot{\epsilon}a_0,\quad \dot{a}_2=-\Phi_2^a \tag{44}$$

$$\dot{a}_3=-\Phi_3^a+\kappa\dot{\epsilon}a_3,\quad \dot{a}_4=-\Phi_4^a-\kappa\dot{\epsilon}a_4. \tag{45}$$

Here we used the dimensionless extensional rate $\dot{\epsilon}=\tau_{\mathrm{ref}}\dot{\epsilon}$.

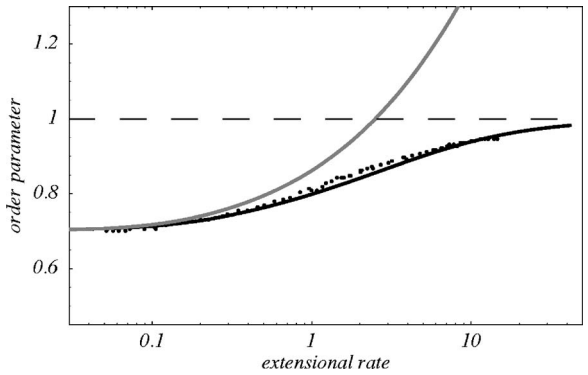

FIG. 3. The average of the scalar order parameter $a=\sqrt{\mathbf{a}:\mathbf{a}}$ calculated numerically is plotted vs the extensional rate $\dot{\epsilon}/6$. The points are the results from the numerical solution of the Fokker-Planck equation obtained in [26]. The orientation increases without limits for the Landau–de Gennes potential (black line), whereas it saturates for the amended potential (gray line). The model parameter are $\lambda_K=1$, $\kappa=0$, and $\vartheta=0$.

In order to compare our results to [26], we scaled the curve as follows. For the amended potential, the maximum of the order parameter is $a_{\max}=2.5$ and, hence, we scaled the order parameter a by a factor 2.5. On the other hand, in [26] the extensional rate is scaled by the diffusion constant D_r, while in Eqs. (43)–(45), $\dot{\epsilon}$ is scaled by τ_{ref}. From the Fokker-Planck equation, it is possible to derive a relation between the diffusion constant and phenomenological coefficients: $6D_r=A\tau_a^{-1}$ [6]. Finally, we used the temperature $\vartheta=-3.67$ such that our equilibrium value of the order parameter coincides with the equilibrium value of Maffettone *et al.* [26].

Figure 3 shows the orientational order parameter as a function of the dimensionless extensional rate $\dot{\epsilon}$. Very good agreement is found between the numerical solution of the Fokker-Planck equation and the alignment tensor theory with the amended potential for all values of the extensional rate. The Landau–de Gennes potential, however, cannot be used for extensional rates $\dot{\epsilon}\gtrsim 1$. Similar results are be obtained for different values of the parameter κ as shown in Fig. 4. For intermediate extensional rates $\dot{\epsilon}\approx 1$, the values of the order parameter differ by roughly 10% for different choices of κ.

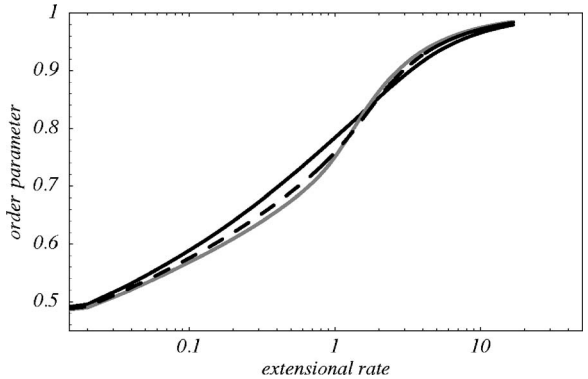

FIG. 4. The average of the scalar order parameter $a=\sqrt{\mathbf{a}:\mathbf{a}}$ as a function of the extensional rate is displayed for different parameter values κ ($\kappa=0.4$ dark curve, $\kappa=0.8$ dashed curve, $\kappa=1$ gray curve). The model parameters are $\lambda_K=4/3$ and $\vartheta=0$.

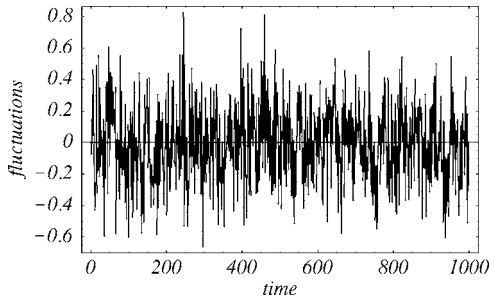

FIG. 5. Pseudorandom fluctuation given by $f(t)$ as a nonlinear function of the time t, Eq. (47).

In the case of shear flow, as will be considered in Sec. VII, the dependence on κ is even smaller as already was pointed out by [7]. Therefore, we choose $\kappa=0$ for further investigations.

VII. ORIENTATIONAL BEHAVIOR FOR FLUCTUATING SHEAR RATES

A. Modeling of fluctuations

In experiments the shear rate cannot be kept absolutely constant. It can be perturbed by the roughness of the shear plates or by the motion of the plates itself. If such fluctuations are very fast compared to the time scale of the orientational dynamics, they can be neglected. Otherwise, shear rate fluctuations should be taken into account in order to make the theoretical analysis more realistic.

In order to study the influence of fluctuations, we consider time-dependent shear rates of the form

$$\dot{\gamma}(t) = \dot{\gamma}_0[1 + \xi f(t)], \tag{46}$$

where $f(t)$ is an analytical function that model Gaussian distributed random numbers with zero mean and variance $\sigma=0.25$. Here, $\dot{\gamma}_0$ is the mean value of $\dot{\gamma}(t)$ and ξ measures the strength or amplitude of noise. The function $f(t)$ is given by

$$f(t) = \frac{1}{5}\left[g(t) + g\left(\frac{t}{10}\right) + g\left(\frac{t}{100}\right) + g\left(\frac{t}{\sqrt{10}}\right) + g\left(\frac{10t}{\sqrt{10}}\right)\right] \tag{47}$$

as a linear combination of the function

$$g(t) = \cos[\pi \sin(\pi t)] \sin\{\pi[t + \sin(e\pi t)]\}. \tag{48}$$

In Fig. 5, the model function $f(t)$ is plotted against the time t. The extremal values for f are ± 1.

Pseudorandom numbers are calculated by $f_i=f(t_i)$ and are approximately Gaussian distributed. In Fig. 6, the distribution is compared to the Gauss function $[\sqrt{2\pi\sigma}]^{-1}\exp-\frac{x^2}{2\sigma^2}$, where $\sigma=0.25$ is the square root of the second cumulant.

On the other hand, in order to test our results, we generate Gaussian-distributed pseudorandom numbers as described in [27]. In Fig. 6, the distribution function of numerically generated pseudorandom numbers is shown.

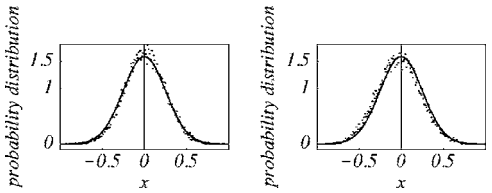

FIG. 6. The distribution function of dimensionless pseudorandom fluctuations x is displayed [left for numerical calculated random numbers and right for random numbers calculated via the nonlinear function $f(t)$].

B. Isotropic phase, flow aligned nematic and periodic solutions

In the isotropic regime, every aligned initial configuration decays to a state with random orientation such that the components of the alignment tensor tend to zero. In order to investigate the effect of shear rate fluctuations on this behavior, we set $\dot{\gamma}(t)=\xi f(t)$. We found no significant qualitative effects of fluctuating shear rates on the dynamical solutions. In Fig. 7, the time evolution of the scalar order parameter $a=\sqrt{\mathbf{a}:\mathbf{a}}$ is shown both in the absence of noise and in the presence of small and strong shear rate fluctuations.

In the nematic phase, the orientational flow leads to enhanced alignment for high values of $\dot{\gamma}$ and λ_K. The molecules show mostly in one preferred direction. Therefore, after a transient period, the components of the alignment tensor reach stationary values. In Fig. 8, the scalar order parameter is plotted as function on time for numerically and analytically generated fluctuations and in the absence of fluctuations. In principle, the solutions with noisy shear rates are not different from the usual solutions. Only some fluctuations on the stationary values of alignment tensor components can be observed. This means that the molecules fluctuate around the preferred direction. In Fig. 8, for example, the time evolution of the alignment tensor component a_1 is shown for $\xi=0$ and $\xi=5.0$.

Periodic solutions occur in a manifold way, depending on the model parameter λ_K and $\dot{\gamma}$, as was discussed in Sec. V. For example, for the parameter $\dot{\gamma}_0=2.0$ and $\lambda_K=0.9$, we have a kayaking tumbling (KT) solution, whereas for $\dot{\gamma}_0=5.0$ and

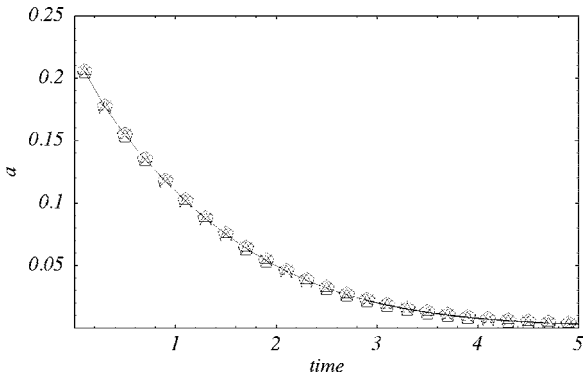

FIG. 7. The scalar order parameter a in the isotropic regime as a function of the time is given for several values of the parameter ξ (pentagonal for $\xi=0$, triangle for $\xi=5$, and cross for $\xi=10$). The reduced temperature is $\vartheta=1$; the model parameters are $\lambda_K=1.0$, $\dot{\gamma}_0$ and $\kappa=0$.

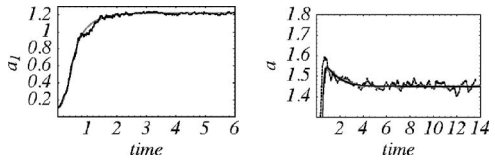

FIG. 8. The time evolution of the scalar order parameter a in the flow alignment regime with fluctuations of the shear rate ($\xi=2.5$) around $\gamma_0=2.0$ calculated numerically and analytically (dashed line) compared to the original solution (gray line, $\xi=0$) (left). The time evolution of the tensor component a_1 in the flow alignment regime for strong fluctuations ($\xi=5.0$) of the shear rate around $\dot{\gamma}_0=2.0$ and in the absence of fluctuations (gray line) is compared (right). The reduced temperature is $\vartheta=0$; the model parameters are $\lambda_K=1.5$ and $\kappa=0$.

$\lambda_K=0.9$ we observe a tumbling (T) solution [7]. One could suspect that strong fluctuations of the shear rate $\dot{\gamma}$ lead to a transition of the KT to the T solution. But we observe that even for the strongest fluctuations investigated, the KT solutions for $\dot{\gamma}_0=2$ persists, despite the fact that the largest values of the shear rates fluctuating around $\dot{\gamma}_0=2$ are in a range where a tumbling solution occurs for stationary shear.

In Fig. 9, we compare orbits of nonfluctuating shear rates with orbits obtained from strong fluctuations ($\xi=50$, $\xi=170$). Again, the trajectory is perturbed by fluctuations, but the character of the solution is conserved. Only at very strong, physically unrealistic fluctuations, does the KT solution change to a noisy wagginglike solution. This observation is the same for both fluctuation types as is shown in Fig. 10.

The robustness of solutions against fluctuations is also observed for other periodic solutions. In Fig. 11, we show phase plots of wagging solutions for several values of ξ. It can be seen that for increasing ξ, the phase cycle is smeared

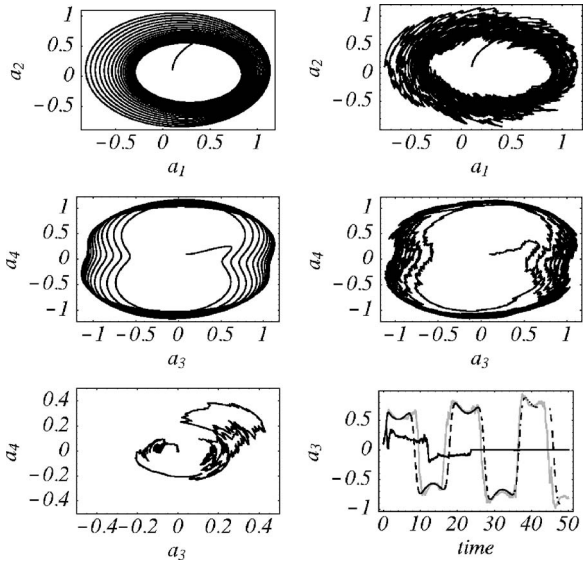

FIG. 9. The orbits a_4 vs a_3, a_2 vs a_1, and the time evolution of a_3 is plotted for several coupling constants: $c=0$ (upper left), $\xi=50$ (upper right) and $\xi=170$ (lower left). In the lower right, the graphs for $\xi=0$ (dashed line), $\xi=50$, and $\xi=170$ (gray line) are displayed. The temperature is $\vartheta=0$; the model parameters are $\lambda_K=1.0$, $\dot{\gamma}_0=1.0$ and $\kappa=0$.

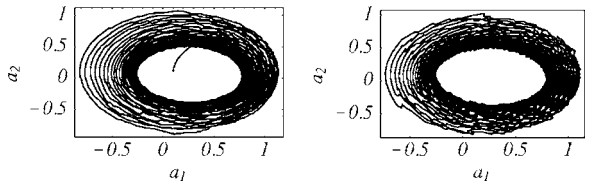

FIG. 10. The orbit a_1 vs a_2 at fluctuation strength $\xi=10$ of the shear rate around $\gamma=1.0$ are displayed. The fluctuations are modelled numerically (left) and analytically (right). The reduced temperature is $\vartheta=0$; the model parameters are $\lambda_K=1.0$ and $\kappa=0$.

out because the rapid distorsion seen in the solution overlaps the original curves. In principle, all orbits show the same response to small and intermediate fluctuations. We conclude, therefore, that fluctuations perturb the trajectory, but the system tries to follow the original dynamic without distorsions (Fig. 12). Only at very high values of the parameter ξ is the dynamical behavior described by the character of the fluctuations, and differences between numerical and analytical calculated noise becomes significant.

C. Robustness of chaotic solutions

It seems obvious that fluctuations affect chaotic solutions because of its sensitivity on changing the model parameter $\dot{\gamma}$ or λ_K. It is astonishing that we found chaotic solutions to be very robust against uncorrelated noise. In order to investigate the effect of shear rate fluctuations on the chaotic solutions, we calculated the largest Lyapunov exponent. For that purpose, the trajectories of the alignment tensor components are perturbed by a small vector $\boldsymbol{d}_0$. After some time steps, the distance between the perturbed and unperturbed trajectory is measured by $\boldsymbol{d}_1$, and the perturbed trajectory is rescaled such that the new distance is $\boldsymbol{d}_0$. The logarithm of the ratio $\boldsymbol{d}_1/\boldsymbol{d}_0$ is calculated. This procedure is repeated for many steps, and the average of the logarithms leads to the largest Lyapunov exponent. The numerical implementation of the algorithm is described in [28].

In Fig. 13, the largest Lyapunov exponent against the fluctuation amplitude is displayed. The Lyapunov exponent is positive for a wide range of the parameter ξ. That means, for

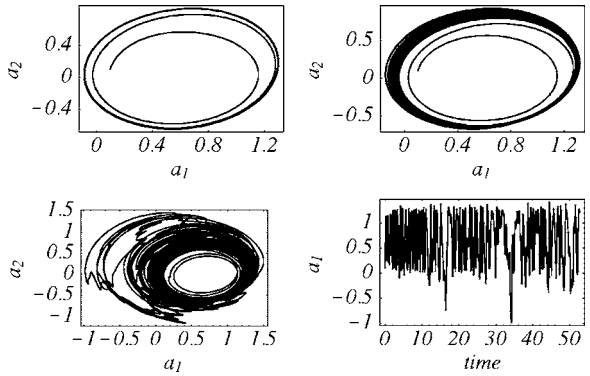

FIG. 11. The orbits a_1 vs a_2 in the tumbling regime for $\xi=0$ upper left, $\xi=1$ upper right, and $\xi=5$ lower left. In the lower right the time evolution of a_1 for $c=5$ is given. The reduced temperature is $\vartheta=0$; the model parameters are $\lambda_K=0.8$, $\dot{\gamma}=6$, and $\kappa=0$.

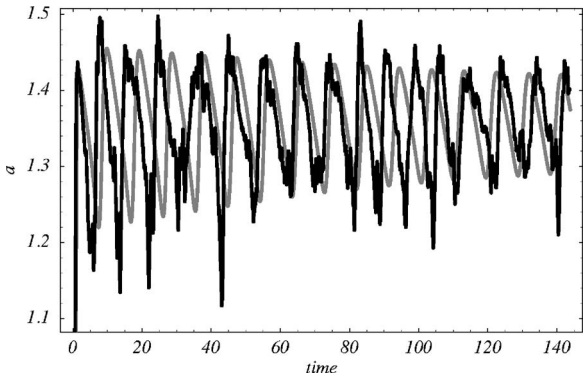

FIG. 12. The time evolution of the scalar order parameter a with (ξ=2.5) and without (gray line) fluctuations. The reduced temperature is ϑ=0; the model parameters are λ_K=1.0, $\dot{\gamma}_0$=1.0, and κ=0.

fluctuations up to 13 times higher than the averaged shear rate, the solution is still chaotic. Such high fluctuations are not realistic for experiments as long as the flow is laminar. Therefore, chaotic behavior is not sensitive against uncorrelated fluctuations of the shear rate in experiments. The same could be observed for fluctuations that were generated by the analytical function $f(t)$ as shown in Fig. 14. Again, fluctuations up to 14 times higher than $\dot{\gamma}_0$ not perturb the chaotic states. Despite the similarities, there is a significant difference between the two plots. In the range between ξ=0 and ξ=6, the Lyapunov exponent increases in the case of numerical calculated fluctuations, whereas if the fluctuations were modeled by the analytic function $f(t)$ it decreases. This can be explained by the fact that the Lyapunov exponent measure the noise if it is chaotic like the fluctuations calculated numerically.

Also, the trajectories of the alignment tensor components are not changed. Figure 15 shows that the trajectory in the phase space is practically not affected even by rather strong fluctuations. The trajectory is only modulated by some noisy distorsions as already noted for periodic solutions.

VIII. CONCLUSIONS

In this paper, we analyzed how fluctuations of the shear rate affect the dynamics of tumbling nematics. We found

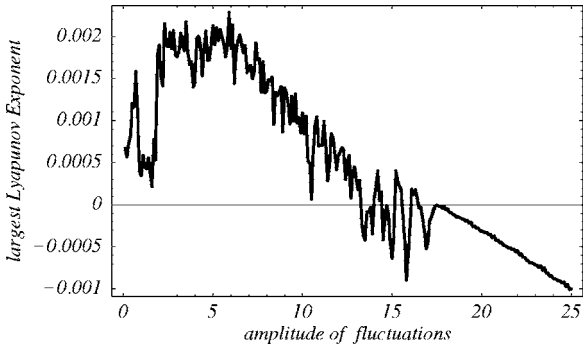

FIG. 13. The largest Lyapunov exponent is plotted against the amplitude of fluctuations ξ. Fluctuations are modeled as Wiener process. The reduced temperature is ϑ=0; the model parameters are λ_K=1.17, $\dot{\gamma}_0$=3.72, and κ=0.

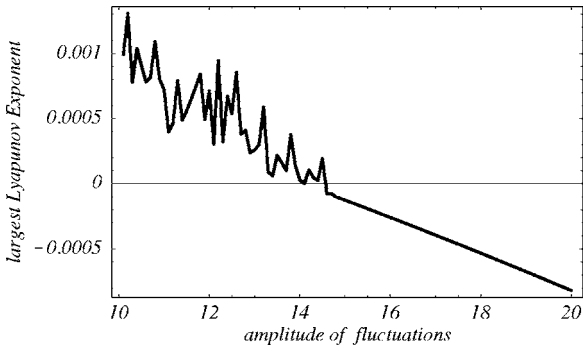

FIG. 14. The largest Lyapunov exponent is plotted against the amplitude of fluctuations ξ, where fluctuations are modeled by Eq. (47). The same parameters as in Fig. 12 are chosen.

that, in general, fluctuations do not change the character of the solutions. Only small distorsions on the trajectory could be observed. This result is the same for both kinds of perturbations investigated as long as the strength of the fluctuations is not too high.

It is surprising that chaotic solutions are very sensitive against the change of averaged shear rate but not on fluctuations. The study of the largest Lyapunov exponent shows that no small parameter values ξ exist such that the chaotic behavior is lost. In the case of periodic solutions, we showed that for increasing fluctuation strength the phase trajectory is smeared out more and more. The orientation of nematic follows the original phase trajectory. Small fluctuations indicate oscillations of the orientation around the original trajectory. In conclusion fluctuations of the shear rate does not affect the dynamics nematic liquid crystals in the shear flow.

This result changes drastically when the velocity gradient fluctuates itself. In [29], Chaubal and Leal could show that a variation of the velocity gradient and its effect on other flow components may destroy the periodic director behavior.

Furthermore, we presented here a potential to model the nematic-to-isotropic transition. Our potential has the advantage to restrict the order parameter to physically admissible values. We sketched how a restricted potential can be derived from Onsager's excluded volume potential. To make the cal-

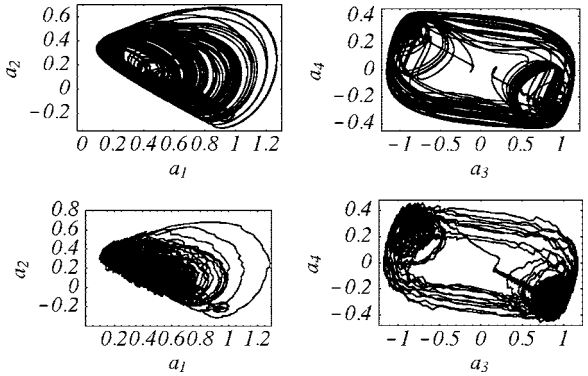

FIG. 15. The orbit a_1 vs a_2 (left) and a_3 vs a_4 (right) in the chaotic regime at mean shear rate γ_0=3.7 for several coupling constants ξ (upper graph ξ=0.05 and lower graph ξ=8). The reduced temperature is ϑ=0; the model parameters are λ_K=1.15 and κ=0.

culations simple, we used the amended model potential for further investigations. This potential not only restricts the order parameter to physically admissible values but also coincides with the Landau–de Gennes potential for small values of the order parameter.

Here we should mention that higher-order terms of the Landau–de Gennes potential lead to more complicated equilibrium phase diagrams. For example, a term proportional to $[Tr(\mathbf{a}^3)]^2$ can be used to describe biaxial nematic phases in equilibrium [30]. However, effects of this kind are not studied here.

The amended model potential leads for shear flows to the same characteristic solutions at shifted model parameters λ_K and $\dot{\gamma}$. This can be explained by the different value of the equilibrium value of the order parameter a_{eq}. The equilibrium value is given by the condition $\phi'(a_{eq})=0$ and therefore depends on the value of a_{max}.

In contrast to plane Couette flow, extensional flows lead to different results. In the case of four-rolls-mill flow, we could show that the amended potential prevents the order parameter from increasing boundlessly. The scalar order parameter values calculated with the relaxation equation including the amended potential coincide with experimental results very well.

In further work, we will use the amended potential to investigate spatially inhomogeneous orientational dynamics of tumbling nematics.

ACKNOWLEDGMENTS

This research has been performed under the auspices of the Sonderforschungsbereich 448 "Mesoskopisch strukturierte Verbundsysteme," financially supported by the Deutsche Forschungsgemeinschaft (DFG).

[1] R. G. Larson, *The Structure and Rheology of Complex Fluids* (Oxford University Press, Oxford, 1999).
[2] S. Hess, Z. Naturforsch. A **30A**, 728 (1975).
[3] S. Hess, Z. Naturforsch. A **31A**, 1507 (1976).
[4] P. D. Olmsted and P. M. Goldbart, Phys. Rev. A **41**, R4578 (1990); **46**, 4966 (1992).
[5] C. Pereira Borgmeyer and S. Hess, J. Non-Equil. Thermodyn. **20**, 359 (1995).
[6] G. Rienäcker, Thesis, TU Berlin, 2000; *Orientational Dynamics of Nematic Liquid Crystals in a Shear Flow* (Shaker Verlag, Aachen, 2000).
[7] G. Rienäcker, M. Kröger, and S. Hess, Phys. Rev. E **66**, 040702(R) (2002); Physica A **315**, 537 (2002).
[8] M. Grosso, R. Keunings, S. Crescitelli, and P. L. Maffettone, Phys. Rev. Lett. **86**, 3184 (2001).
[9] M. G. Forest, Q. Wang, and R. Zhou, Rheol. Acta **86**, 80 (2004); S. M. Fielding and P. D. Olmsted, Phys. Rev. Lett. **92**, 084502 (2004); B. Chakrabarti, M. Das, C. Dasgupta, S. Ramaswamy, and A. K. Sood, *ibid.* **92**, 055501 (2004).
[10] S. Hess and M. Kröger, J. Phys.: Condens. Matter **16**, S3835 (2004); in *Computer Simulations Bridging Liquid Crystals and Polymers*, edited by P. Pasim, C. Zannoni, and S. Zumer (Kluwer, Dordrecht, 2005), p. 295.
[11] G. G. Fuller, *Optical Rheometry of Complex Fluids* (Oxford University Press, New York, 1995).
[12] S. Hess and I. Pardowitz, Z. Naturforsch. A **36A**, 554 (1981).
[13] G. Marrucci and F. Greco, Mol. Cryst. Liq. Cryst., **206**, 17 (1991); M. Kröger and H. S. Sellers, in *Complex Fluids*, edited by L. Garrido, Lecture Notes in Physics Vol. 415 (Springer, New York, 1992), p. 295; G. Sgalari, G. L. Leal, and J. J. Feng, J. Non-Newtonian Fluid Mech. **102**, 361 (2002).
[14] S. Hess and P. Ilg, Rheol. Acta **44**, 465 (2005); P. Ilg and S. Hess, J. Non-Newtonian Fluid Mech. **134**, 2 (2006).
[15] G. Rienäcker and S. Hess, Physica A **267**, 294 (1999).
[16] S. Hess, Z. Naturforsch. A **31A**, 1034 (1976).
[17] S. Hess, in *Electro-Optics and Dielectrics of Macromolecules and Colloids*, edited by B. R. Jennings (Plenum, New York, 1979).
[18] M. Doi, Ferroelectrics **30**, 247 (1980); J. Polym. Sci., Polym. Phys. Ed. **19**, 229 (1981).
[19] C. Schneggenburger, M. Kröger, and S. Hess, J. Non-Newtonian Fluid Mech. **62**, 235 (1996).
[20] J. L. Ericksen, Trans. Soc. Rheol. **5**, 23 (1961); F. M. Leslie, Arch. Ration. Mech. Anal. **28**, 265 (1968).
[21] G. B. Jeffrey, Proc. R. Soc. London, Ser. A **102**, 171 (1922).
[22] J. Feng, C. V. Chaubal, and L. G. Leal, J. Rheol. **42**, 1095 (1998).
[23] D. R. J. Chillingworth, E. V. Alonso, and A. A. Wheeler, J. Phys. A **34**, 1393 (2001).
[24] P. Ilg, I. V. Karlin, and H. C. Öttinger, Phys. Rev. E **60**, 5783 (1999).
[25] P. Kaiser, W. Wiese, and S. Hess, J. Non-Equil. Thermodyn. **17**, 153 (1992).
[26] P. L. Maffettone, M. Grosso, M. C. Friedenberg, and G. G. Fuller, Macromolecules **29**, 8473 (1996).
[27] W. T. Vetterling, S. A. Teukolsky, W. H. Press, and B. P. Flannery, *Numerical Recipes in Fortran 77: The Art of Scientific Computing* (Cambridge University Press, Cambridge, England, 1992), p. 274.
[28] G. Benettin, L. Galani, A. Giorgilli, and J. M. Strelcyn, Meccanica **15**, 9 (1980).
[29] C. V. Chaubal and G. L. Leal, J. Non-Newtonian Fluid Mech. **82**, 25 (1999).
[30] E. F. Gramsbergen, L. Longa, and W. H. de Jeu, Phys. Rep. **135**, 195 (1986).